Journal of Molecular Structure 1141 (2017) 469–476

Contents lists available at ScienceDirect

Journal of Molecular Structure

journal homepage: http://www.elsevier.com/locate/molstruc

Substituent and intramolecular hydrogen-bond effect on the fluorescent emission of two easy-synthesizable fused rigid bicyclic octadiene derivatives

Víctor Muñoz [a], Sebastián Cumsille [b], Germán Günther [c], Nancy Pizarro [b], Andrés Vega [a, *]

[a] Universidad Andrés Bello, Facultad de Ciencias Exactas, Departamento de Ciencias Químicas, Av. República 498, Santiago, Chile
[b] Universidad Andrés Bello, Facultad de Ciencias Exactas, Departamento de Ciencias Químicas, Quillota 980, Viña del Mar, Chile
[c] Universidad de Chile, Facultad de Ciencias Químicas y Farmacéuticas, Departamento de Química Orgánica y Fisicoquímica, Sergio Livingstone 1007, Santiago, Chile

ARTICLE INFO

Article history:
Received 24 February 2017
Received in revised form
27 March 2017
Accepted 29 March 2017
Available online 5 April 2017

Keywords:
Bicyclo octadiene
Hydrogen-bond
Weak emission

ABSTRACT

Tetra-*tert*-butyl-*cis,cis*-3,7-dihydroxybicyclo[3.3.0]octa-2,6-diene-2,4-*exo*-6,8-*exo*-tetracarboxylate (**I**) and tetra-*tert*-butyl-*cis,cis*-3,7-dimethoxybicyclo[3.3.0]octa-2,6-diene-2,4-*exo*-6,8-*exo*-tetracarboxylate (**II**) were prepared in a three step synthetic procedure. These compounds show two central five carbon atom rings, fused in such a way to define a central bicyclo[3.3.0]octa-2,6-diene core. The carbon atoms which fuse both rings have sp^3 hybridization, then they are not coplanar. A dihedral angle of about 63° corresponds to butterfly conformation. UV–Vis spectra of **I** and **II** measured in solution show symmetrical bands centred around 245 nm ($\varepsilon \sim 10^4$ $M^{-1}cm^{-1}$). These bands are consistent with $\pi \rightarrow \pi^*$ transitions. TD-DFT simulated spectra over the DFT optimized in gas phase confirms this hypothesis, and additionally suggest a non-negligible contribution of $n \rightarrow \pi^*$ transition for **II**. The slight dependence of λ_{max} on solvent polarity experimentally observed for **II** is consistent with some $n\pi^*$ character. After excitation at 250 nm, a weak emission around 400 nm was detected for both compounds, with quantum yield values below detection limit for **I**. The value of λ_{em} of **II** was observed to be sensible to the solvent polarity, confirming some relevant $n \rightarrow \pi^*$ character. The almost fully quenching of the emission of **I** in solution would be attributed to a rather strong intramolecular hydrogen bond established between the hydroxyl group and the oxo-oxygen atom from tert-butoxy group, which is observed in the crystal structure of the compound (O···O ranges from 2.635(2) Å to 2.672(2) Å). We hypothesize that it is probably preserved in solution due to the molecular rigidity, and would be the responsible for the quenching of the emission in solvent solution.

1. Introduction

Fused bicyclic rings are useful frameworks with several synthetic applications, using them as synthons, bridged cores or building block systems [1–4]. Interesting optical properties or photochemistry reactions have focused attention on these systems [5–9]. In particular, bicyclo[3.3.0]octa-2,6-dienes are easily prepared by the reaction of α-diketones with 3-oxoglutarate esters, being valuable precursors for organic synthesis. The use of this family of molecules strongly depends on the possibility to functionalize them through nucleophilic substitution, by removing one the two-acidic protons located in the carbon bicycle with a strong base (i.e. sodium hydride) and the subsequent reaction with an alkyl or aryl halide. However, since there are two equivalent positions in the molecule, the control of the reaction is difficult, even at low temperatures, a mixture of products, which is hard or even impossible to separate, is obtained [10]. An elegant way to overcome this issue, is to take advantage of steric hindrance on the carboxylate substituents. Even though they are not directly involved in the reaction, the use of a big substituent allows driving the reaction to a single product, simplifying isolation and purification for the further steps of synthesis.

Although the wide use of them as a part of synthetic routes, rather a handful have been fully structurally characterized. The structure of the Vossen's salt $C_{16}H_{15}O_{10}Na$, prepared by the first

* Corresponding author.
E-mail address: andresvega@unab.cl (A. Vega).

http://dx.doi.org/10.1016/j.molstruc.2017.03.123
0022-2860/

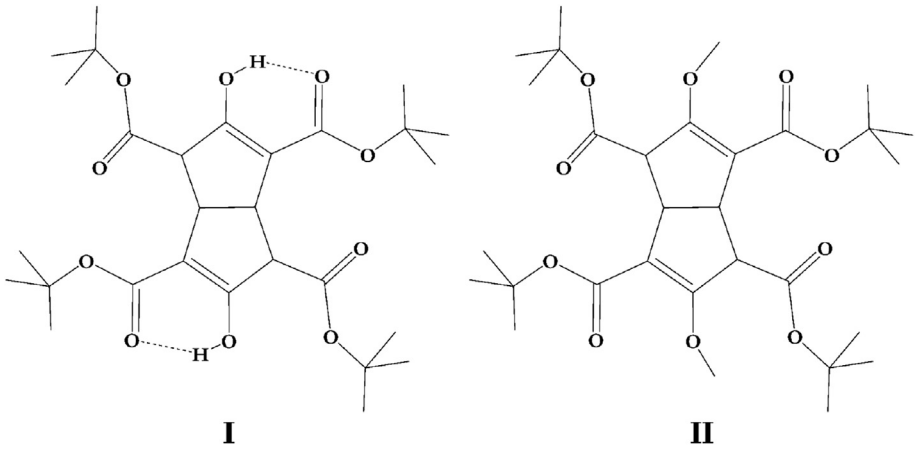

Scheme 1. Schematic view of **I** (*left*) and **II** (*right*).

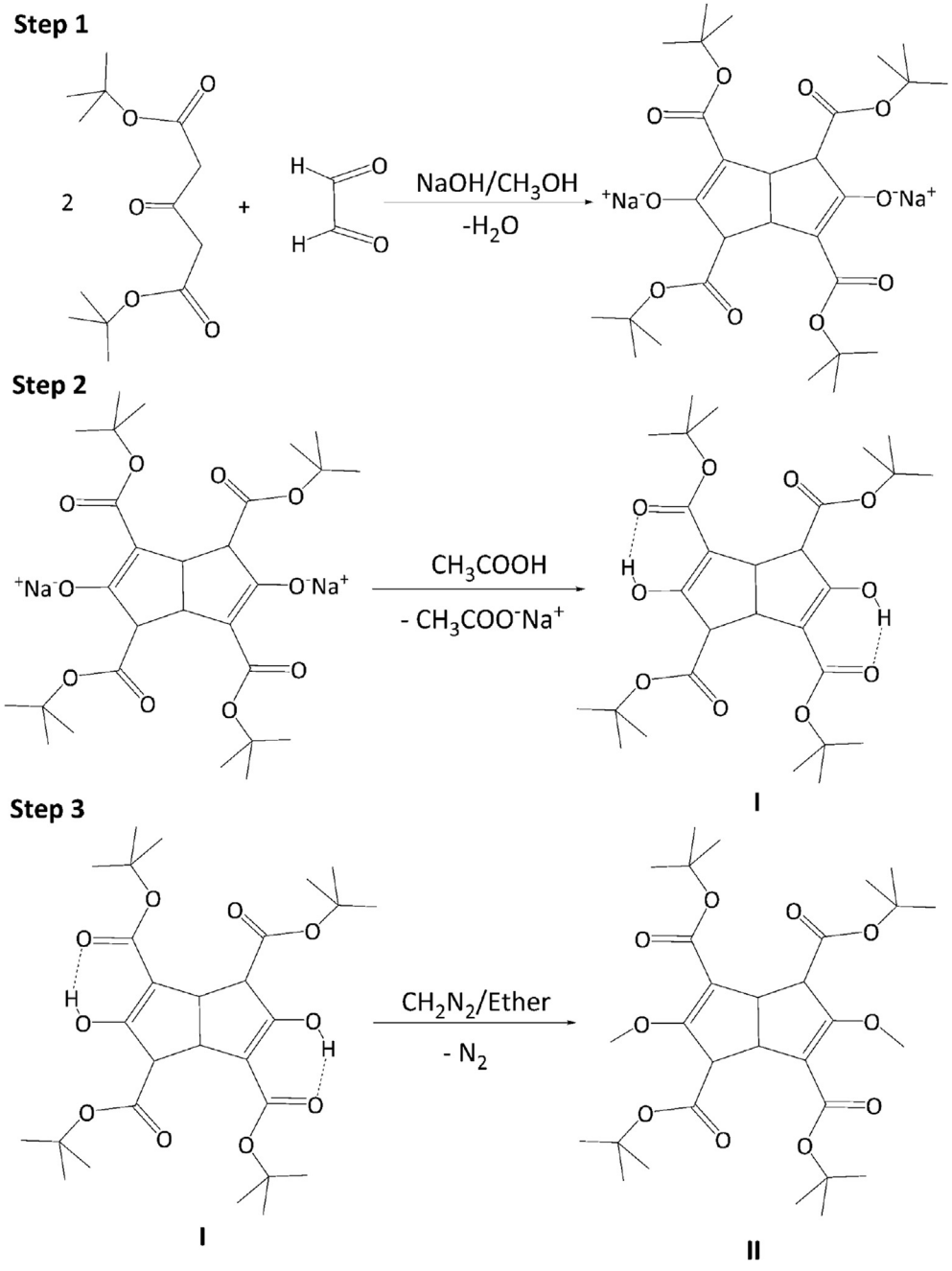

Scheme 2. Synthetic path to **II.**

time in 1910 [11], was reported just in 2002 [12]. The structure of related compounds with different substitution patterns have been recently published [13–15].

Taking this in mind, we present in this report the structure of tetra-*tert*-butyl-*cis,cis*-3,7-dihydroxybicyclo-[3.3.0]octa-2,6-diene-2,4-*exo*-6,8-*exo*-tetracarboxylate (**I**) and tetra-*tert*-butyl-*cis,cis*-3,7-dimethoxybicyclo-[3.3.0]octa-2,6-diene-2,4-*exo*-6,8-*exo*-tetracarboxylate (**II**), and discuss on the differences with related molecules (Scheme 1). Evidence from photo-physical behaviour of these molecules in terms of their respective structures allows us to identify the main electronic transitions involved, with $\pi \rightarrow \pi^*$ and $n \rightarrow \pi^*$ character for compounds **I** and **II**, respectively. In addition, we attribute their weak fluorescent emission to their non-planar structure, and moreover, the complete quench of the emission of compound **I** in solvent solution at room temperature due to the presence of an intramolecular hydrogen bond.

2. Experimental

2.1. Synthesis

The synthesis follows the previously reported protocol of Bertz et al. [16], slightly modified in order to avoid the formation sticky by-products [14]. Methylation using diazomethane also followed a previously described protocol [14]. Standard Schlenck techniques and nitrogen inert atmosphere were used for all manipulations. Reagents were used as received. The synthesis of **II** occurs in three steps, with **I** as an intermediate, as shown in Scheme 2.

2.1.1. Step 1, synthesis of tetra-tert-butyl-cis,cis-3,7-dihydroxybicyclo[3.3.0]octa-2,6-diene-2,4-exo-6,8-exo-tetracarboxylate disodium salt

1.59 g of NaOH were dissolved in 50 ml of methanol and then filtered. This solution was mixed with 10.00 g of di-*tert*-butylacetonedicarboxylate in 50 ml of methanol. To this boiling solution, 3.58 g of glyoxal in 10 ml of methanol were added dropwise. Solution was kept boiling for 15 m after the end of the addition. After cooling, the sodium salt was filtered off from the solution and washed with small portions of cold methanol. 11.1 g of product were obtained, 98.3% yield.

2.1.2. Step 2, synthesis of tetra-tert-butyl-cis,cis-3,7-dihydroxybicyclo[3.3.0]octa-2,6-diene-2,4-exo-6,8-exo-tetracarboxylate (I)

The disodium salt was quantitatively transformed into tetra-*tert*-butyl-cis-3,7-hidroxy-bicyclo[3.3.0]octa-2,6-diene-cis-2,4-*exo*-6,8-*exo*-tetracarboxylate by dissolving in water and adding dropwise a 1.0 M solution of acetic acid. Recrystallization from ethyl-acetate yields a pure microcrystalline colourless solid.

^{1}HRMN (δ, $CDCl_3$): 1.470 (s, 3H), 1.510 (s, 3H), 3.490 (s, 1H), 3.731 (s, 1H), 10.600 (s, 1H). ^{13}CRMN (δ, $CDCl_3$): 28.219 (s), 28.556 (s), 43.784 (s), 56.939 (s), 81.963 (s), 82.209 (s), 105.125 (s), 169.269 (s), 170.549 (s), 171.227 (s). (*m/z*) (Rel. int.): 538.33 $[M]^+$ (2), 482.26 (4), 426.18 (12), 370.11 (25), 314.04 (100), 296.02 (76), 278.01 (57).

2.1.3. Step 3, synthesis of tetra-tert-butyl-cis,cis-3,7-dimethoxybicyclo[3.3.0]octa-2,6-diene-2,4-exo-6,8-exo-tetracarboxylate (II)

Compound **I** was quantitatively methylated at the hydroxy group by using diazomethane in cold diethylether solution. The dimethyl derivative was isolated in its pure form after evaporation of diethylether. X-rays quality crystals of the compound were obtained by recrystallization in methanol.

^{1}HNMR (δ, C_3D_6O): 1.487 (s, 3H), 1.496 (s, 3H), 3.627 (s, 1H), 3.634 (d, J = 1.49 Hz, 1H), 3.634 (d, J = 1.47 Hz, 1H). ^{13}CRMN: (δ, C_3D_6O): 28.33 (s), 28.68 (s), 47.33 (s), 57.30 (s), 59.44 (s) 80.63 (s), 82.25 (s), 111.16 (s), 163.96 (s), 165.22 (s), 171.80 (s). (*m/z*) (Rel. int.): 566.34 $[M]^+$ (2), 510.28 (1), 454.20 (11), 436.19 (41), 380.12 (9), 324.05 (33), 306.03 (100).

2.2. UV–vis and fluorescence spectroscopies

UV–vis spectra were recorded on an Agilent 8453 diode-Array spectrophotometer in the range of 250–600 nm in a series of organic solvents. Experiments were carried out in either air-equilibrated and argon-saturated solutions. Emission spectra were measured in a Horiba Jobin-Yvon FluoroMax-4

Table 1
Crystal data and structure refinement details for **I** and **II**.

	I	II
FW/uma	538.62	566.67
Crystal System	Triclinic	Orthorhombic
Space Group	$P\bar{1}$	$P2_12_12_1$
a (Å)	11.888(4)	13.101(5)
b (Å)	14.599(4)	14.034(6)
c (Å)	18.466(6)	17.813(7)
α (°)	108.162(7)	90
β (°)	90.244(8)	90
γ (°)	98.613(7)	90
V (Å^3)	3006.4(16)	3275(2)
Z(Z′)	2(4)	4(4)
d (g cm^{-3})	1.190	1.149
μ (mm^{-1})	0.090	0.085
F(000)	1160	1224
θ range	1.162 to 25.99	1.847 to 26.00
hkl range	$-14 \le h \le 14$	$-16 \le h \le 16$
	$-18 \le k \le 18$	$-17 \le k \le 17$
	$-22 \le l \le 22$	$-21 \le l \le 21$
N_{tot}, N_{uniq} (R_{int}), N_{obs}	23440, 11739 (0.0704), 7084	24318, 6432 (0.0820), 5648
Refinement Parameters	714	375
GOF	1.441	1.052
R1, w*R*2 (obs)	0.1641, 0.2159	0.0448, 0.1215
R1, w*R*2 (all)	0.3985, 0.4337	0.0512, 0.1290
Max. and minΔρ	1.296 and −0.406	0.263 and −0.270

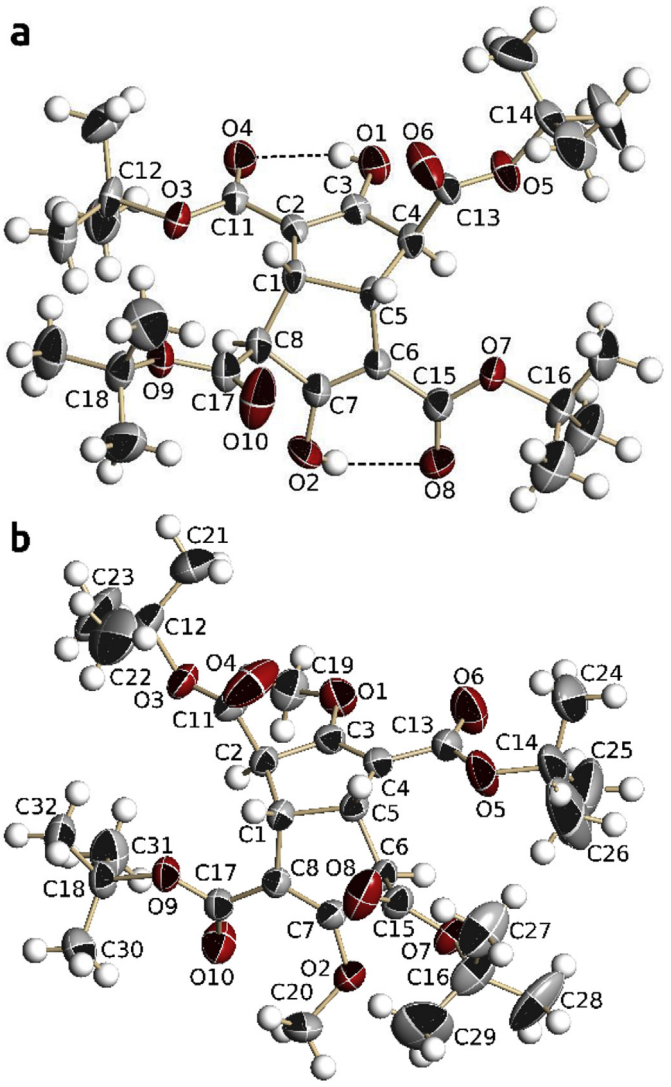

Fig. 1. Molecular structure diagram for **a.- Ia** and **b.- II**. Partial atom numbering scheme is included. Displacement ellipsoids drawn at the 50% level of probability.

spectrofluorometer in different solvents at room temperature and in EtOH/MeOH glass (4:1, v/v) at 77 K. Emission quantum yields (Φ_{em}) were measured at room temperature using quinine sulphate in 0.1 M H_2SO_4 (Φ_{em} = 0.546 for excitation at 350 nm) as actinometer [17]. The optical densities of the sample (OD_x) and actinometer (OD_{std}) solutions were set below 0.10 and matched at the excitation wavelength. The quantum yield of the sample was calculated by using Eq. (1)

$$\varnothing_x = \varnothing_{std}\frac{I_x}{I_{std}}\left(\frac{OD_{std}}{OD_x}\right)\left(\frac{\eta_x}{\eta_{std}}\right)^2 \quad (1)$$

Table 2
Hydrogen-bond geometry (Å, °) for **I**.

D–H···A	D···A	D–H···A
Ia		
O2–H2···O8	2.667(6)	138
O1–H1···O4	2.623(6)	117
Ib		
O101–H101···O104	2.622(6)	125
O102–H102···O108	2.686(6)	140

Table 3
Summary of main energy, wavelength and oscillator strength computed for observed transitions in the absorption spectra of **I** and **II**.

N	E/eV	λ/nm	*f*	Major Contributions
I				
1	4.47	277	0.004	HOMO → LUMO (95%)
5	4.96	250	0.378	HOMO-1 → LUMO+1 (27%)
				HOMO → LUMO+1 (26%)
				HOMO-1 → LUMO (25%)
6	5.12	242	0.005	HOMO-4 → LUMO (58%)
				HOMO-1 → LUMO+1 (19%)
II				
1	4.55	273	0.086	HOMO → LUMO (78%)
5	4.92	252	0.227	HOMO-1 → LUMO+1 (48%)
6	5.12	242	0.220	HOMO-1 → LUMO+1 (27%)
				HOMO-3 → LUMO+1 (20%)

where $\varnothing_{std}$ is the known quantum yield of the actinometer, I_x and I_{std} are the integrated fluorescence intensities for the sample and actinometer, and η_x and η_{std} are the refractive index of sample and actinometer solutions.

Luminescence lifetime measurements were carried out in a PicoQuant FluoTime 300 fluorescence lifetime spectrometer with time correlated single photon counting technique. A PLS-280 sub-nanosecond Pulsed LED was employed as the pulsed light source (FWHM ~ 500 ps; pulse energy 1 μW).

2.3. X-rays diffraction

The crystal structure of both compounds was determined by X-rays diffraction at 293 K. Data collection were made on a SMART CCD diffractometer using ϕ and ω-scans as data collection strategy. Data set was reduced with SAINT [18], while the structure was solved by direct methods and completed by Difference Fourier Synthesis. Least-squares refinement were conducted by using SHELXL [19,20]. Multi-scan absorption corrections were applied using SADABS [18]. The hydrogen atoms positions were calculated after each cycle of refinement with SHELXL using a riding model for each structure, with C–H distance of 0.93–0.98 Å. U_{iso}(H) values were set equal to 1.2 U_{eq} or 1.5 U_{eq} of the parent carbon atom. Table 1 shows additional structural and refinement details for the compound. The final indices for the refinement of **I** would be attributed to the effect of a non-fully corrected twining of the

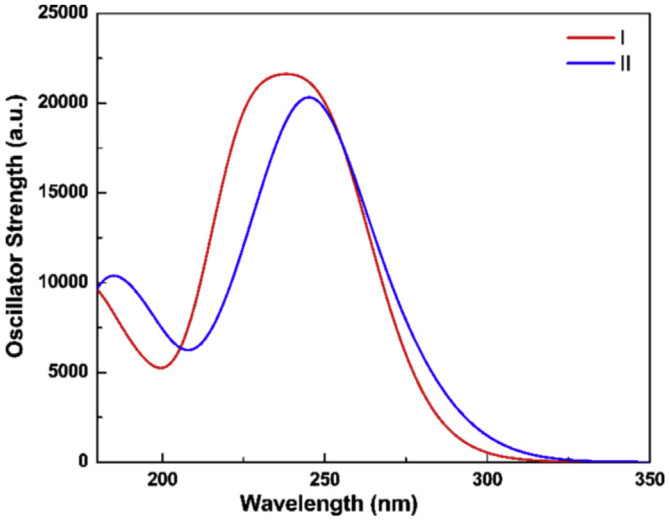

Fig. 2. TD-DFT computed excitations for **I** (–) and **II** (–) in gas phase.

crystals. Efforts to improve this results, including redetermination and re-crystallization, failed. Although the structure is confidently determined, with very meaningful values for interatomic distances, angles or U's, should be considered of poor quality. The structure of **I** display two independent and non-crystallographically related molecules of the compound, subsequently denominated as **Ia** and **Ib** where necessary. Hydroxyl hydrogen atoms on **I** were computed based on geometrical considerations (O–H = 0.82 Å) since confident location from Difference Fourier map give no meaningful result. Tables were prepared by using Publcif [21].

2.4. Computational details

All geometry optimizations were performed at the B3LYP/6-31 + G(d,p) level of theory using the Gaussian09 Rev C.01 package of programs (G09) [22], and started from geometry determined by means of X-rays diffraction. Excited state calculations were performed within the time-dependent DFT methodology as implemented in G09. Absorption and emission spectra were simulated from the above calculations using the GaussSum 3.0 suite of freely available processing tools. A full width at half-maximum (FWHM)

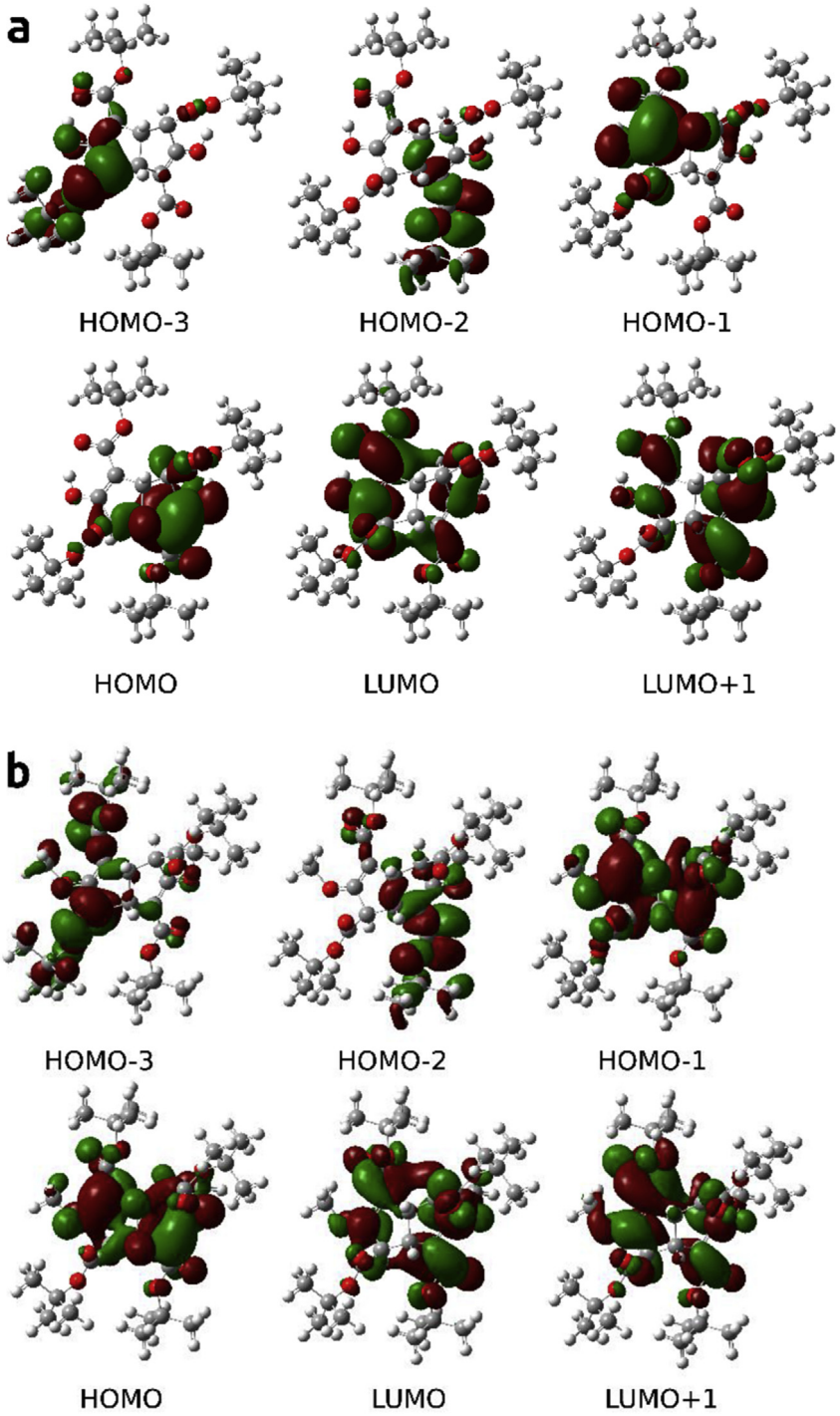

Fig. 3. DFT computed frontier orbitals HOMO-3, HOMO-2, HOMO-1, HOMO, LUMO and LUMO+1 plots for **a.- I** and **b.- II**.

of the Gaussian curves corresponding to 3000 cm^{-1} was employed to convolute both spectra. Representations for molecular orbitals were generated using the G09 cubegen tool and have been visualized using VMD and Povray 3.6 programs [23,24].

3. Discussion

3.1. Structural description

The compounds (Scheme 1), are constructed, as the related compounds of the family, over the central bicyclo[3.3.0]octa-2,6-diene core. Each one of the two carbon rings of the bicyclic core are almost planar, although, since they are fused through sp^3-hybridized carbon atoms, they are not coplanar. The dihedral angle defined by the two least-squares planes is 63.1° (average **Ia** and **Ib**) for **I** and 63.7(1)° for **II** respectively, then the core could be well described having a butterfly geometry as clear from Fig. 1a and b. Table S1 (Supporting Information) show the most relevant distances, angles and torsion angles for the compounds. This conformation for the central bicyclic core makes both faces of the molecule inequivalent. Considering this, the tert-butoxy carbonyl groups over carbon atoms C4 and C8 display an *exo* conformation, as observed for the methoxycarbonyl related molecule [14].

The methoxy groups substituting the bicycle at carbons C3 and C7 are rather coplanar with the ring where they are attached, as reflected by the rather low values measured for the C—C—O—C torsion angles. But, in contrast to that observed for tetramethyl-*cis,cis*-3,7-dihydroxybicyclo[3.3.0]octa-2,6-diene-2,4-*exo*,6,8-*exo*-tetracarboxylate, the methyl groups display a cis-conformation, with both at the same side of the plane which divides the molecule in halves passing across the methoxy oxygen atoms.

The hydroxyl hydrogen atoms on each side of the bicyclooctadiene core of **I** define intramolecular hydrogen bonds with the oxo-oxygen atoms from the neighbouring carboxylate group connected through a double bond to the hydroxyl carbon atom. This allows the required proximity for hydrogen bonds. Moreover, the resulting electronic conjugation of the carboxylate to the double bond would be rigid enough to preserve the H-bond in solution. The *exo*-conformation of the other carboxylate group prevent hydrogen bond occur to that. Details are shown in Table 2, with O···O distance around 2.6 Å. As previously observed for tetramethyl-*cis,cis*-3,7-dihydroxybicyclo[3.3.0]octa-2,6-diene-2,4-*exo*-6,8-*exo*-tetracarboxylate and tetramethyl-*cis,cis*-3,7-dihydroxy-1,5-dimethylbicyclo[3.3.0]octa-2,6-diene-2,4-*exo*-6,8-*exo*-tetracarboxylate, where O···O distances range between 2.635(2) Å and 2.672(2) Å, this indicates rather strong interactions [25].

3.2. Computational results

To get deeper insight of the behaviour of this system, we performed TD-DFT calculations in gas phase over the DFT geometry optimized of **I** and **II**.

There are no significant differences between the optimized distances and those determined. Table 3 summarizes the energy of the computed transitions by means of TD-DFT, while Fig. 2 shows the simulated spectra for the molecule in gas phase. Fig. 3, **a** and **b**, shows the frontier and near frontier orbitals for **I** and **II**, as computed from DFT geometry optimization. For both cases the HOMO and LUMO have π character.

Results on Table 3 and Fig. 3 show that the absorption in the UV—Vis region at lower energy involves mainly π → π* transition for compound **I**, while for **II**, a higher contribution of the n → π* transition can be found, due to the larger methoxy contribution to the HOMO (Fig. 3b).

3.3. Photophysical properties

Absorption spectra of **I** and **II** in solution are shown in Fig. 4. Symmetrical absorption bands were observed for both compounds centred around 245 nm, the high molar extinction coefficients ($\varepsilon \sim 10^4\ M^{-1}cm^{-1}$), allow to attribute them to a π→π* transitions.

The absorption band of compound **II** was slightly more sensible to solvent polarity, showing a maximum displacement to lower energies in polar solvents like MeCN or MeOH, while absorption maxima of Compound **I** was independent on solvent polarity. This difference can be explained due to a major n→π* character of involved transition for **II**. The red-shifted absorption band of **I** in comparison with **II**, could be attributed to the intramolecular hydrogen bond, which would reduce the HOMO-LUMO gap.

Upon excitation at 250 nm, emission band was detected for compound **II**, but just a weak emission for **I**. This last one with emission quantum yield below the detection limit our equipment (see Table 4). Maximum wavelength of emission band of **II** (around 400 nm) was also sensible to solvent polarity. These results are in agreement with the major n→π* character of involved transition for **II**. The weak emission of compound **I** in solution could be explained in terms of the intramolecular hydrogen bond

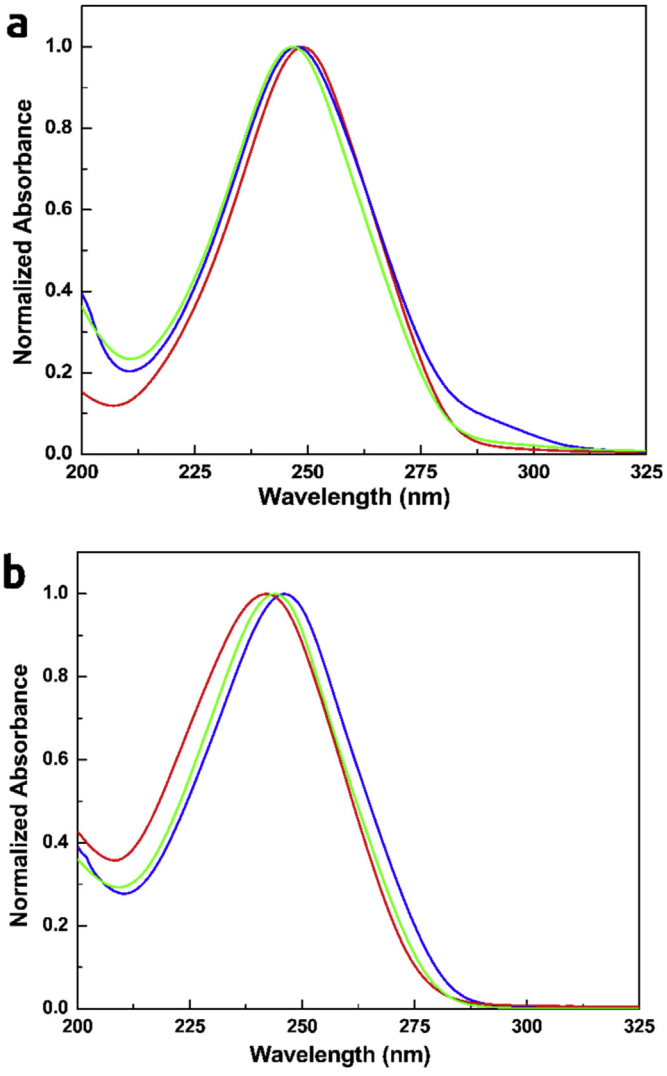

Fig. 4. Absorption spectra for **a.- I** and **b.- II** in solution of: (—) MeCN, (—) MeOH and (—) Hexane.

Table 4
Summary of some photophysical properties for **I** and **II** in solution at 298 K and in glassy solution at 77 K.

Solvent	I		II	
	λ_{abs} (nm), ε ($M^{-1}cm^{-1}$)	λ_{em} (nm), Φ_{em}	λ_{abs} (nm), ε ($M^{-1}cm^{-1}$)	λ_{em} (nm), Φ_{em}
MeCN	247, 18900	<0.001	244, 21700	400, 0.006
MeOH	248, 19300	<0.001	246, 20600	399, 0.006
Hex	249, 17600	<0.001	242, 18500	<0.001
EtOH:MeOH(77 K)	–	445	–	392

established between the hydroxyl and the ester groups in the molecule, which would contribute with additional vibrational modes, and also, producing the red-shift of the energy transition [26]. At low temperature, in glassy solution at 77 K (See Figure 5a), an increment of the emission intensity for both compounds was observed. The emission maxima for **I** is around 50 nm red-shifted in comparison with the one for **II**. Time-resolved emission measurements at room temperature (See Figure 5b) allow us to obtain the fluorescent lifetimes for **I** and **II**. Biexponential emission decays were obtained with average amplitude weighted lifetime values of 2.21 for **I** and 3.22 ns for **II**. Short fluorescence lifetimes have been observed for similar compounds [27].

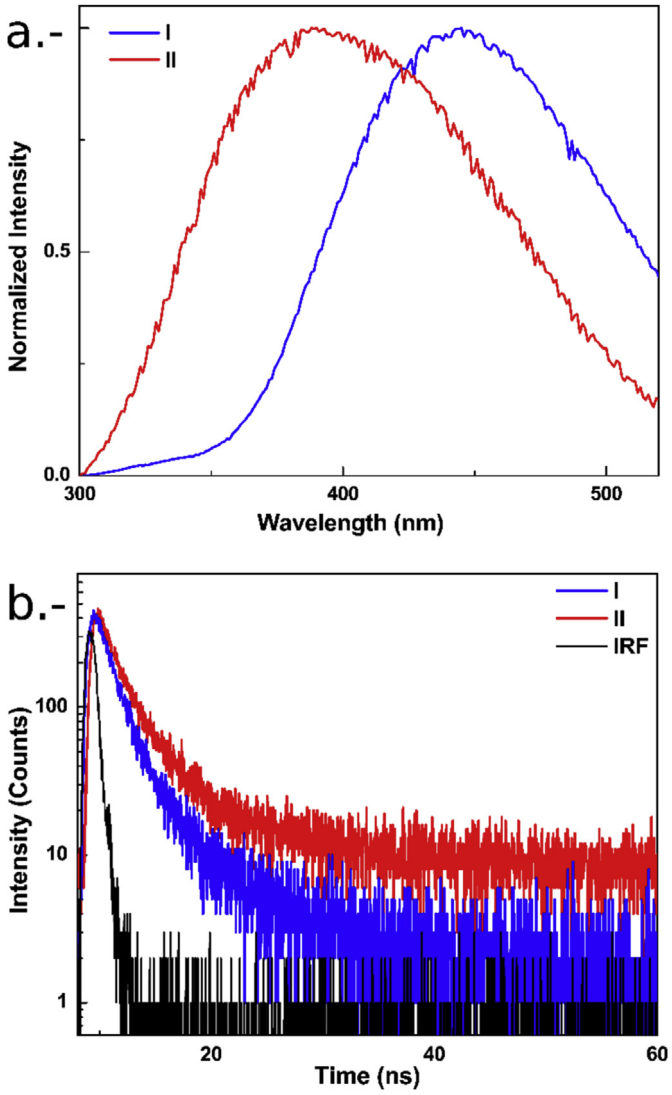

Fig. 5. a.- Emission spectra for **I** and **II** in glassy solution at 77 K **b.-** Emission decay for **I** and **II** in MeCN solution at 298 K upon excitation at 280 nm.

4. Conclusion

The fused rigid bicyclic octadiene derivatives **I** and **II** were easily prepared in a three-step synthetic procedure. These compounds show two central five carbon atom rings, fused in such a way to define a central bicyclo[3.3.0]octa-2,6-diene core. The carbon atoms which fuse both rings have sp^3 hybridization, then they are not coplanar. A dihedral angle of about 63° corresponds to butterfly conformation. Evidence from photophysical behaviour of these molecules in terms of their respective structures allows us to identify the involved main electronic transitions with $\pi \rightarrow \pi^*$ and $n \rightarrow \pi^*$ character for compound **I** and **II**, respectively. In addition, we attribute their weak fluorescent emission to their rigid butterfly non-planar structure, and moreover, the total quench of the fluorescent emission for compound **I** at room temperature would be attributed to the presence of the intramolecular hydrogen bonds among the hydroxyl and the ester groups in the molecule.

Acknowledgements

The authors gratefully acknowledge financial support from Fondecyt 11060176 and PicoQuant for the special discount of FluoTime300.

Appendix A. Supplementary data

Supplementary data related to this article can be found at http://dx.doi.org/10.1016/j.molstruc.2017.03.123.

References

[1] M. Presset, Y. Coquerel, J. Rodriguez, Syntheses and applications of functionalized Bicyclo[3.2.1]octanes: thirteen years of progress, Chem. Rev. 113 (1) (2013) 525–595.
[2] K.A. Parker, Y.-H. Lim, "Endo" and "exo" bicyclo[4.2.0]-octadiene isomers from the electrocyclization of fully substituted tetraene models for SNF 4435C and D. Control of stereochemistry by choice of a functionalized substituent, Org. Lett. 6 (2) (2004) 161–164.
[3] C.-H. Lai, Y.-L. Shen, M.-N. Wang, N.S. Kameswara Rao, C.-C. Liao, Intermolecular Diels–Alder reactions of brominated masked o-benzoquinones with electron-deficient dienophiles. A detour method to synthesize Bicyclo[2.2.2]octenones from 2-methoxyphenols, J. Org. Chem. 67 (18) (2002) 6493–6502.
[4] M.A. Filatov, F. Etzold, D. Gehrig, F. Laquai, D. Busko, K. Landfester, S. Baluschev, Interplay between singlet and triplet excited states in a conformationally locked donor-acceptor dyad, Dalton Trans. 44 (44) (2015) 19207–19217.
[5] H.R. McAlexander, T.D. Crawford, Simulation of circularly polarized luminescence spectra using coupled cluster theory, J. Chem. Phys. 142 (15) (2015) 154101.
[6] G. Bagdžiūnas, E. Butkus, S. Stončius, Homoconjugation vs. exciton coupling in chiral α,β-unsaturated Bicyclo[3.3.1]nonane dinitrile and carboxylic acids, Molecules 19 (2014) 9893–9906.
[7] V. Singh, S. Pal, S.M. Mobin, Cycloaddition between electron-deficient π-systems, photochemical and radical-induced reactions: a novel, general, and stereoselective route to polyfunctionalized bridged Bicyclo[2.2.2]octanes, Bicyclo[3.3.0]octanes, Bicyclo[4.2.0]octanes, and Tricyclo[4.3.1.03,7]decanes, J. Org. Chem. 71 (8) (2006) 3014–3025.
[8] M.-S. Yang, S.-S. Lu, C.P. Rao, Y.-F. Tsai, C.-C. Liao, Photochemistry of bicyclo [2.2.2]oct-7-ene-2,5-diones and the corresponding 5-hydroxyimino and 5-methylene derivatives, J. Org. Chem. 68 (17) (2003) 6543–6553.
[9] T.A. Zeidan, S.V. Kovalenko, M. Manoharan, R.J. Clark, I. Ghiviriga, I.V. Alabugin, Triplet acetylenes as synthetic equivalents of 1,2-bicarbenes: phantom n,π* state controls reactivity in triplet photocycloaddition, J. Am. Chem. Soc. 127 (12) (2005) 4270–4285.
[10] A.K. Gupta, X. Fu, J.P. Snydert, J.M. Cook, General approach for the synthesis of polyquinenes via the Weiss reaction, Tetrahedron 47 (23) (1991) 3665–3710.
[11] G. Schroeter, Untersuchungen über hydrierte Naphthaline und deren Umwandlungen, Justus Liebigs Ann. Chem. 426 (1–2) (1922) 1–17.
[12] D. Djaidi, R. Bishop, D.C. Craig, M.L. Scudder, Schroeter and Vossen's red salt revealed, New J. Chem. 26 (5) (2002) 614–616.

[13] R. Vaughan Williams, V.R. Gadgil, A. Vij, J.M. Cook, G. Kubiak, Q. Huang, Unexpected stereoselectivity in the Weiss-Cook condensation of dimethyl 1,3-acetonedicarboxylate with pentane-2,3-dione, J. Chem. Soc. Perkin Trans. 1 (9) (1997) 1425–1428.
[14] A. Vega, O. Donoso-Tauda, A. Ibañez, C.A. Escobar, Five bicyclo[3.3.0]octa-2,6-dienes, Acta Crystallogr. Sect. C 64 (4) (2008) o199–o204.
[15] J. Gao, M.M. Bhadbhade, R. Bishop, Different crystal forms of a rich hydrogen bond acceptor compound resulting from alternative C-H···O and orthogonal C=O···C=O molecular interaction patterns, CrystEngComm 14 (1) (2012) 138–146.
[16] S.H. Bertz, G. Rihs, R.B. Woodward, Reaction of dimethyl sodio-3-ketoglutarate with glyoxal and substituted glyoxals, Tetrahedron 38 (1) (1982) 63–70.
[17] G.A. Crosby, J.N. Demas, Measurement of photoluminescence quantum yields. Review, J. Phys. Chem. 75 (8) (1971) 991–1024.
[18] APEX2, Bruker AXS Inc., Madison, Wisconsin, USA, 2001.
[19] G. Sheldrick, A short history of SHELX, Acta Crystallogr. Sect. A 64 (1) (2008) 112–122.
[20] G. Sheldrick, Crystal structure refinement with SHELXL, Acta Crystallogr. Sect. C 71 (1) (2015) 3–8.
[21] S. Westrip, publCIF: software for editing, validating and formatting crystallographic information files, J. Appl. Crystallogr. 43 (4) (2010) 920–925.
[22] M.J.T. Frisch, G.W. Trucks, H.B. Schlegel, G.E. Scuseria, M.A. Robb, J.R. Cheeseman, G. Scalmani, V. Barone, B. Mennucci, G.A. Petersson, H. Nakatsuji, M. Caricato, et al., Gaussian 09, Gaussian, Inc., Wallingford CT, 2009.
[23] W. Humphrey, A. Dalke, K. Schulten, VMD: visual molecular dynamics, J. Mol. Graph. 14 (1) (1996) 33–38.
[24] Persistence of Vision (TM) Raytracer, Persistence of Vision Pty. Ltd., Williamstown, Victoria, Australia, 2004.
[25] G.R. Desiraju, Hydrogen bridges in crystal engineering: interactions without borders, Acc. Chem. Res. 35 (7) (2002) 565–573.
[26] T. Lin, X.J. Liu, Z.D. Lou, Y.B. Hou, F. Teng, Intermolecular-charge-transfer-induced fluorescence quenching in protic solvent, J. Mol. Struct. 1123 (2016) 49–54.
[27] C.-Y. Wang, Y.-S. Yeh, E.Y. Li, Y.-H. Liu, S.-M. Peng, S.-T. Liu, P.-T. Chou, A new class of laser dyes, 2-oxa-bicyclo[3.3.0]octa-4,8-diene-3,6-diones, with unity fluorescence yield, Chem. Commun. 25 (2006) 2693–2695.